J. Am. Soc. Mass Spectrom. (2016) 27:1468–1475
DOI: 10.1007/s13361-016-1420-2

RESEARCH ARTICLE

A Radical-Mediated Pathway for the Formation of $[M + H]^+$ in Dielectric Barrier Discharge Ionization

Jan-Christoph Wolf,[1] Luzia Gyr,[1] Mario F. Mirabelli,[1] Martin Schaer,[2] Peter Siegenthaler,[2] Renato Zenobi[1]

[1]Department of Chemistry and Applied Bioscience, ETH Zurich, CH-8093, Zurich, Switzerland
[2]Federal Office for Civil Protection FOCP, Spiez Laboratory, Analytical Chemistry Branch, CH-3700, Spiez, Switzerland

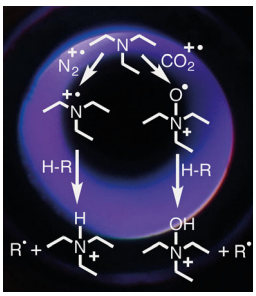

Abstract. Active capillary plasma ionization is a highly efficient ambient ionization method. Its general principle of ion formation is closely related to atmospheric pressure chemical ionization (APCI). The method is based on dielectric barrier discharge ionization (DBDI), and can be constructed in the form of a direct flow-through interface to a mass spectrometer. Protonated species ($[M + H]^+$) are predominantly formed, although in some cases radical cations are also observed. We investigated the underlying ionization mechanisms and reaction pathways for the formation of protonated analyte ($[M + H]^+$). We found that ionization occurs in the presence and in the absence of water vapor. Therefore, the mechanism cannot exclusively rely on hydronium clusters, as generally accepted for APCI. Based on isotope labeling experiments, protons were shown to originate from various solvents (other than water) and, to a minor extent, from gaseous impurities and/or self-protonation. By using CO_2 instead of air or N_2 as plasma gas, additional species like $[M + OH]^+$ and $[M - H]^+$ were observed. These gas-phase reaction products of CO_2 with the analyte (tertiary amines) indicate the presence of a radical-mediated ionization pathway, which proceeds by direct reaction of the ionized plasma gas with the analyte. The proposed reaction pathway is supported with density functional theory (DFT) calculations. These findings add a new ionization pathway leading to the protonated species to those currently known for APCI.

Keywords: DBDI, Ionization mechanism, Active capillary plasma ionization, APCI, Radical mediated protonation, Hydronium clusters

Received: 22 March 2016/Revised: 12 May 2016/Accepted: 13 May 2016/Published Online: 5 July 2016

Introduction

An important question in modern mass spectrometry concerns the origin and the reaction pathway of the charging species, frequently a proton. This is of fundamental interest in plasma-based and related atmospheric pressure ionization methods, since protonated molecules ($[M + H]^+$) are predominantly observed in positive ion mode [1]. It is commonly believed that the protons originate from hydronium and/or solvent clusters [1–5], according to Kebarle's water displacement reaction (Equation 1) [6]:

$$\left[(H_2O)_nH\right]^+ + M \rightarrow \left[M(H_2O)_{n-1}H\right]^+ + H_2O \quad (1)$$

The $[M(H_2O)_{n-1}H]^+$ clusters then undergo a desolvation step to form the observed $[M + H]^+$ ion. Accordingly, the current understanding of the ionization mechanism for all plasma-based ionization methods [e.g. APCI, direct analysis in real time (DART), or the low temperature plasma probe (LTP)] is centered on the formation of hydronium [7] clusters from excited or ionized gas molecules [8–11]:

$$He^* + nH_2O \rightarrow \left[(H_2O)_{n-1}H\right]^+ + OH^- + He \quad (2)$$

Jan-Christoph Wolf and Luzia Gyr contributed equally to this work.

Electronic supplementary material The online version of this article (doi:10.1007/s13361-016-1420-2) contains supplementary material, which is available to authorized users.

Correspondence to: Jan–Christoph Wolf; *e-mail:* j.c.wolf@gmx.ch, Renato Zenobi; *e-mail:* zenobi@org.chem.ethz.ch

$$N_4^{+\bullet} + H_2O \rightarrow 2N_2 + H_2O^{+\bullet} \quad (3)$$

Apart from the proton transfer model described above, an additional hypothesis for the formation of protonated species exists for atmospheric pressure photoionization (APPI) [12]. This model assumes a direct ionization of the analyte either by electron ionization (Equation 4) or by charge transfer from ionized plasma gas (Equation 5), followed by a hydrogen atom transfer from the solvent (Equation 6):

$$M + e^- \rightarrow M^{+\bullet} + 2e^- \quad (4)$$

$$M + N_2^{+\bullet} \rightarrow M^{+\bullet} + N_2 \quad (5)$$

$$M^{+\bullet} + H_2O \rightarrow [M + H]^+ + OH^{\bullet} \quad (6)$$

This mechanism is well accepted for APPI. In APCI, it is believed that only nonpolar compounds, such as polycyclic aromatic hydrocarbons (PAH) or benzene, form radical cations via this mechanism [8, 9]. For the formation of protonated polar molecules, the hydronium cluster model is used exclusively in the literature for both plasma-based or APCI-like ambient ionization techniques [13]. One reason for this is the solvent dependence of the APCI process, which was described by a couple of research groups [14, 15]. Because the ionization efficiency was found to depend on the solvent, the direct ionization pathway was disregarded in mechanistic investigations, since a solvent-independent behavior would have been expected [16]. However, this neglects the possibility that both mechanisms contribute (proton transfer and/or direct ionization followed by a hydrogen atom transfer). After decades of experience with APCI and the development of a vast number of new APCI-like ionization methods [17], there is still insufficient experimental evidence regarding the actual protonation pathways and their contribution to the formation of $[M + H]^+$. An improved understanding of the ionization mechanism would therefore allow the enhancement of APCI-like ambient ionization methods for the detection of specific compounds and for increased sensitivity.

Active capillary plasma ionization [18] is a novel dielectric barrier discharge-based ambient ionization method, where the source itself serves as the interface to the mass spectrometer. In addition to the extraordinary sensitivity [19], this design greatly facilitates mechanistic investigations, since the whole sample passes through the plasma and the reaction time of the analyte and the gas is well defined. In order to study the underlying APCI pathways, we investigated the ionization efficiency of various substances (homologous series of tertiary alkyl amines, phosphonates) in different deuterated solvents, and in a variety of atmospheres (air, N_2, CO_2).

Experimental

Chemicals and Solvents

Diethyl ethylphosphonate (DEEP) (98%), methanol-d (99%) triethylamine (TEA) (>99.5%), tripropylamine (TPrA) (98%), and tributylamine (TBuA) (99%) were obtained from Sigma-Aldrich Chemie GmbH (Buchs, Switzerland). Tripentylamine (TPeA) (99%) and D_2O (99.9%) were purchased from Acros Organics (Geel, Belgium); trihexylamine (THA) (99%) from Alfa Aesar GmbH and Co. KG (Karlsruhe, Germany); ethanol-d (99%), benzene-d_6 (99.5%), and chloroform-d (99.8%) from Cambridge Isotope Laboratories Inc. (Tewksbury, MA, USA). All chemicals were used without further purification. Individual and combined stock solutions (2000 µg/mL each) were prepared in the corresponding solvents. Depending on the experiment, diluted samples were generated from these stock solutions with varying concentrations.

MS Instrumentation

The mass spectra were acquired using Thermo LTQ Orbitrap and LCQ DECA XP mass spectrometers (both from Thermo Scientific, San Jose, CA, USA) fitted with an active capillary plasma ionization source. All spectra were recorded in positive polarity.

Active Capillary Plasma Ionization Source

The principle of the active capillary plasma source has already been described in detail in previous reports [18, 19]. Briefly, a quartz glass capillary (i.d. 0.7 mm, o.d. 1.0 mm) was connected to the inlet of the mass spectrometer. The constant underpressure in the instrument ensured a fixed flow rate of 1.5 L/min through the capillary. A stainless steel capillary (i.d. 0.5 mm, o.d. 0.6 mm) inserted into the glass capillary served as first electrode. The counter-electrode was a 5-mm-long copper ring (i.d. 1.0 mm) surrounding the capillary. By applying a sine modulated (5750 Hz) high voltage (1.5–2.5 kV, peak to peak) to the electrodes, the plasma was ignited inside the capillary by a dielectric barrier discharge, which then ionizes the passing air and sample molecules. All this was enclosed in a gas-tight housing, enabling a direct, leak-tight connection to the plasma gas stream.

Sample Generation

The gas-phase sample generation system was similar to the one used in previous studies [20]. Briefly, a pressurized sample reservoir was connected via a fused silica capillary (ID 40 µm) to a hollow heating cartridge held at 200 °C. The sample outflow was evaporated within the cartridge by temperature and a preheated 3 L/min plasma gas stream, controlled by a mass flow controller. The outlet of the heating cartridge was connected by a T-piece to the active capillary plasma ionization source. The other (excess) outlet is directed to the exhaust. The whole sample generation system is leak-tight and can be fed with different plasma gas streams and sample solutions.

Gas-Phase Sample Delivery

Dry air and dry N_2 plasma gas was prepared by additionally drying the supply gases (purity 4.5) over columns filled with phosphorous pentoxide (Reagent plus 99%, Sigma-Aldrich Chemie GmbH, Buchs, Switzerland) followed by an active charcoal filter. Humidification was done by passing the plasma gas streams through a glass fritted bubbler filled with H_2O or D_2O, respectively. Two mass flow controllers (Bronkhorst High Tech B.V., Ruurlo, The Netherlands) ensured constant flow rates and mixing ratios. Relative humidity was measured using a FHA 646R capacitive humidity sensor and ALMEMO 2590A readout (Ahborn GmbH, Holzkirchen, Germany).

Computational Details

For quantum mechanical calculations, full geometry optimization with no constraints, and frequency calculation for reactants, intermediates, and products were performed with density functional theory (DFT) using the hybrid B3LYP functional as implemented in the GAUSSIAN09 [21] code. For all atoms, the 6-311++G(3df,3pd) basis set was used. For integration, an "ultrafine" grid corresponding to 99 radial shells and 590 angular points per shell was used for increased accuracy, with "tight" optimization criteria. In addition, calculation of the intrinsic reaction coordinates (IRC) for each reaction pathway was performed to show the connection between reactants, products, and the corresponding transition states along the imaginary mode of vibration. All energy values reported in this work are free energies at a temperature of 298 K. For all reactions, the sum of the energies of the separated reactants was set to zero as common reference point.

Results and Discussion

In order to elucidate the ionization mechanism leading to $[M + H]^+$ in plasma-based or APCI-like ambient ionization techniques, the active capillary plasma ionization source [19] was used. It features a fully enclosed ionization volume and precisely controllable gas-phase conditions. The plasma gas, the solvent, and the humidity are the three dominant chemical factors in the plasma that influence the ionization of the analyte in normal operation of the active capillary plasma ionization source. The impact of each of these factors on the $[M + H]^+$ ion formation was studied in this work.

In a first experiment, a homologous series of tertiary alkylamines was ionized in different atmospheres (air, N_2, CO_2) in order to investigate the role of the plasma gas in the ion formation process. The protonated amine ($[M + H]^+$) was the most abundant ion in all atmospheres, even under dry (<100 ppm H_2O) conditions (Figure 1, top).

A direct comparison of the measurements using dry air and CO_2 as plasma gas revealed additional signals with a nominal mass difference of m/z + 17 and m/z – 1 with respect to the monoisotopic mass of the amines (Figure 1, middle). These signals correspond to the protonated and oxidized analyte $[M + OH]^+$ and to the $[M - H]^+$ ion, as additionally confirmed by MS^2 experiments. The latter is most likely formed by hydride abstraction (further discussed below). The fact that these species are observed exclusively in CO_2 atmosphere and neither in

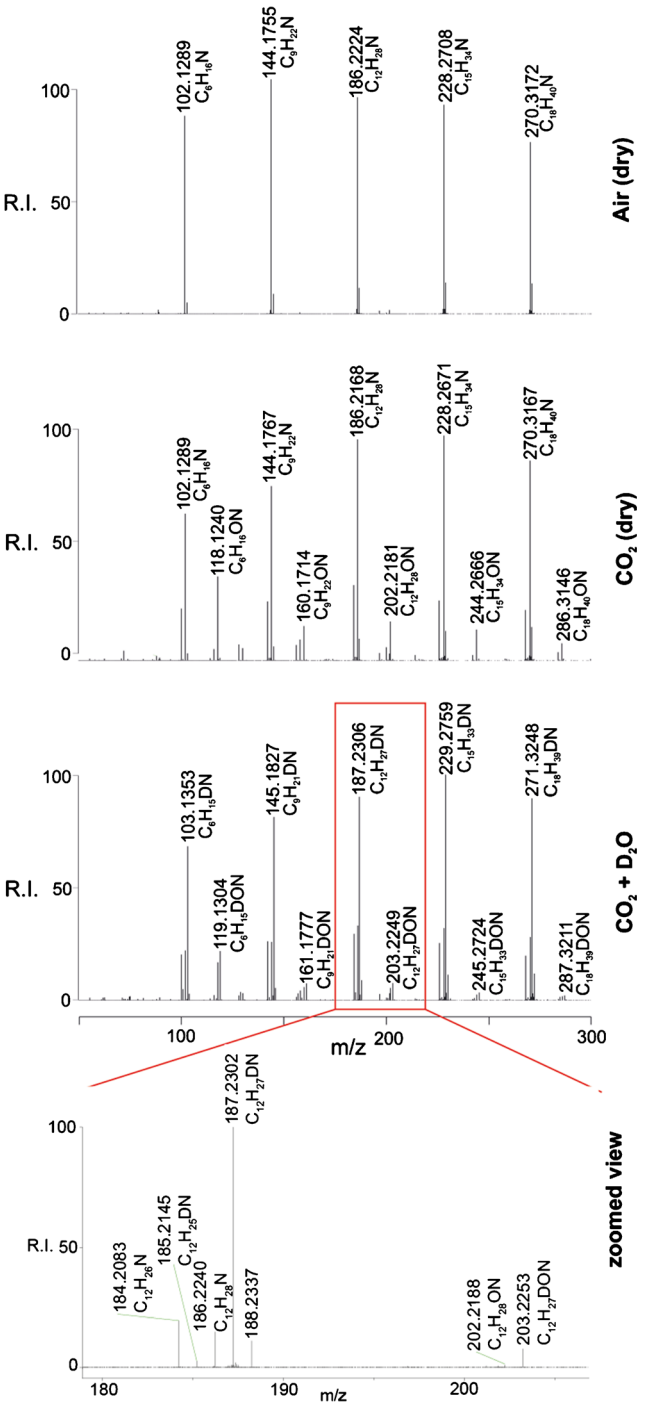

Figure 1. Mass spectra of a trialkylamine (C_2-C_6) mixture measured with the active capillary plasma ionization source under identical conditions in dry air (top), dry CO_2 (middle), and D_2O saturated CO_2 (bottom). The bottom panel part is a zoomed view showing the tributylamine signals (m/z 180–205). Spectra were recorded on an LTQ Orbitrap instrument running in high-resolution mode

N_2 (Supplementary Figure 1) nor in air atmosphere (Figure 1, top) under identical conditions suggests that there is a reaction with CO_2. The ionization potential of CO_2 (318 kcal/mol [22]) is similar to that of N_2 (359 kcal/mol [22]), which is known to be the main constituent in a He and/or in a N_2 plasma [11, 16, 23, 24]. Therefore, the reactive species in a CO_2 plasma can be assumed to be the $CO_2^{+\bullet}$ radical cation. The additional species observed in the mass spectra with CO_2 as plasma gas cannot be explained by the classic proton transfer reaction, but may most easily form in a radical driven pathway, as described for APPI [12]: the protonated oxidized amine ($[M + OH]^+$) can be formed by the reaction of a tertiary amine (M) with a $CO_2^{+\bullet}$ radical cation (Equation 7) or by the reaction of a $M^{+\bullet}$ ion with neutral CO_2 (Equation 8), followed by hydrogen atom transfer from a hydrogen source such as water, leaving an $OH^\bullet$ radical (Equation 9).

$$CO_2^{+\bullet} + M \rightarrow [M + O]^{+\bullet} + CO \quad (7)$$

$$CO_2 + M^{+\bullet} \rightarrow [M + O]^{+\bullet} + CO \quad (8)$$

$$[M + O]^{+\bullet} + H_2O \rightarrow [M + OH]^+ + OH^\bullet \quad (9)$$

The formation of $[M - H]^+$ can be explained by different pathways. Either by direct hydride abstraction from the amine (M) reacting with $CO_2^{+\bullet}$ (Equation 10), by hydrogen radical transfer from the amine radical cation ($M^{+\bullet}$) to CO_2 (Equation 11), by elimination of water from the $[M + OH]^+$ ion (Equation 12), or by elimination of H_2 from the $[M + H]^+$ ion (Equation 13).

$$CO_2^{+\bullet} + M \rightarrow [M{-}H]^+ + CO_2H^\bullet \quad (10)$$

$$CO_2 + M^{+\bullet} \rightarrow [M{-}H]^+ + CO_2H^\bullet \quad (11)$$

$$[M + OH]^+ \rightarrow [M{-}H]^+ + H_2O \quad (12)$$

$$[M + H]^+ \rightarrow [M{-}H]^+ + H_2 \quad (13)$$

In order to determine which reaction pathway is energetically favored, the activation energies ($\Delta G^\ddagger$) and the reaction free energies (ΔG_R) were calculated for all these reactions by DFT. $\Delta G^\ddagger$ and ΔG_R values for triethylamine, tributylamine, and trihexylamine can be found in Table 1. In the following, only the values for tributylamine will be discussed. According to our calculations, the observed $[M + OH]^+$ ion may only be formed through the reaction of $CO_2^{+\bullet}$ with a neutral amine molecule (Equation 7) followed by a hydrogen atom transfer from the solvent (Equation 9), resulting in a net energy gain of roughly –52 kcal/mol (Equations 7 + 9) . The inverse reaction pathway, starting with the reaction of a $M^{+\bullet}$ ion with neutral CO_2 (Equations 8 + 9) is energetically demanding (+103.4 kcal/mol) and thus unlikely. Further proof for a direct reaction of $CO_2^{+\bullet}$ with the analyte comes from the observation of the $[M - H]^+$ ion. Here, several formation pathways are possible. An elimination of H_2 from the protonated molecule $[M + H]^+$ according to reaction (Equation 13) is unlikely (+9 kcal/mol). The direct reaction between M and $CO_2^{+\bullet}$ (Equation 10) is most likely due to a one-step reaction and an energy gain of –113.6 kcal/mol. The inverse reaction, a radical cation $M^{+\bullet}$ reacting with CO_2 (Equation 11) had a similar activation energy, but the reaction free energy is positive (42 kcal/mol). However, also the elimination of water (Equation 12) from $[M + OH]^+$ is possible (–52 kcal/mol), but less favored, since it would involve a reaction chain of three steps (Equations 7 + 9 + 12). The direct reaction (Equation 10) of $CO_2^{+\bullet}$ with the analyte is the preferred reaction for the $[M - H]^+$ ion formation, as also shown in the energy diagram in Figure 2, which includes all four possible reactions. Overall, the energy gain is higher for the formation of $[M - H]^+$ than for $[M + OH]^+$, thus resulting in a higher abundance of $[M - H]^+$ in the mass spectrum, which is,

Table 1. The activation energy ($\Delta G^\ddagger$) and the reaction free energy (ΔG^R) were calculated with DFT (B3LYP/6-311++G(3df,3pd)) for possible reactions in a CO_2 atmosphere with triethylamine (black), tributylamine (red), and trihexylamine (blue). All values are given in kcal/mol, with the sum of the energies of the separated reactants set to zero as common reference point

Reaction	Reaction number	$\Delta G^\ddagger$	ΔG_R
$M + e^- \rightarrow M^{+\bullet} + 2\,e^-$	(4)	/	167.4
		/	161.0
		/	159.3
$CO_2^{+\bullet} + M \rightarrow [M+O]^{+\bullet} + CO$	(7)	97.4	-60.2
		96.7	-64.9
		100.4	-66.6
$CO_2 + M^{+\bullet} \rightarrow [M+O]^{+\bullet} + CO$	(8)	101.6	88.8
		104.2	90.5
		104.4	90.6
$[M+O]^{+\bullet} + H_2O \rightarrow [M+OH]^+ + OH^\bullet$	(9)	17.7	12.0
		18.9	12.9
		19.2	13.1
$CO_2^{+\bullet} + M \rightarrow [M-H]^+ + CO_2H^\bullet$	(10)	54.4	-108.0
		56.1	-113.6
		56.2	-115.2
$CO_2 + M^{+\bullet} \rightarrow [M-H]^+ + CO_2H^\bullet$	(11)	56.8	41.0
		58.3	41.7
		58.6	41.9
$[M+OH]^+ \rightarrow [M-H]^+ + H_2O$	(12)	51.0	-50.5
		50.2	-52.2
		50.1	-52.4
$[M+H]^+ \rightarrow [M-H]^+ + H_2$	(13)	82.8	8.2
		82.0	7.1
		81.9	6.9
$CO_2^{+\bullet} + M \rightarrow M^{+\bullet} + CO_2$	(14)	/	-149.0
		/	-155.4
		/	-157.1
$M^{+\bullet} + H_2O \rightarrow [M+H]^+ + OH^\bullet$	(16)	37.9	30.1
		40.2	32.1
		40.6	32.4

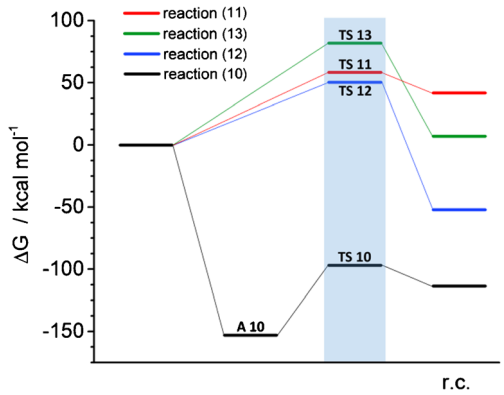

Figure 2. The free energy diagram of the different reactions (Equations 10–13) for the ion formation of $[M–H]^+$ of tributylamine, as calculated by DFT. TS corresponds to the transition state. Reaction 10 has an energy gain in the adduct formation (A10) of $CO_2^{+\bullet}$ with the analyte (M)

except for triethylamine (due to an overlap of isobaric fragment ions), in agreement with our experimental results.

Regardless whether the direct reduction or the water elimination prevails, the formation of all these ions observed and discussed above requires an initial reaction of the ionized plasma gas with the analyte. This is in contradiction to the current APCI model, where the pathway to the protonated molecules always involves reaction of the plasma gas with H_2O.

Revisiting the initial question regarding the formation of the $[M + H]^+$ ion, the initial reactions (Equation 3) and (Equation 5) were compared by using $CO_2^{+\bullet}$ as the reactive species. The formation of the amine radical cation (Equation 14) is strongly favored due to an energy gain of –155 kcal/mol (Table 1) versus –25.8 kcal/mol (Equation 15).

$$CO_2^{+\bullet} + M \rightarrow M^{+\bullet} + CO_2 \quad (14)$$

$$CO_2^{+\bullet} + H_2O \rightarrow H_2O^{+\bullet} + CO_2 \quad (15)$$

$$M^{+\bullet} + H_2O \rightarrow [M + H]^+ + OH^{\bullet} \quad (16)$$

Despite this and the occurrence of less favored reaction products with $CO_2^{+\bullet}$, no $M^{+\bullet}$ species are observed in the spectra, leaving only one explanation: $M^{+\bullet}$ ions are formed but rapidly react further to form $[M + H]^+$, although, according to the calculations, the final reaction (Equation 16) is endothermic for water as hydrogen source. However, one has to consider the clustering processes or other hydrogen sources (e.g., organic solvent, impurities, and other analyte molecules).

The $[M + H]^+$, $[M + OH]^+$, and $[M – H]^+$ ions were also observed under humid conditions, as shown by a repetition of the experiment in a D_2O enriched atmosphere (80% relative humidity, D_2O, Figure 1 bottom). Most, (around 90%) but not all, protons were exchanged by deuterium and therefore originate from solvent molecules, which supports reactions 9 and 16 (endothermic according to our calculations). This is confirmed by high-resolution measurements, as shown in detail for tributylamine (Figure 1, zoomed view). The signals at *m/z* 184.2083 must correspond to $[M – H]^+$, *m/z* 185.2145 to $[M – 2H + D]^+$, *m/z* 186.2240 to the protonated molecule $[M + H]^+$, *m/z* 187.2302 to the deuterated molecule $[M + D]^+$, *m/z* 202.2188 to the oxidized and protonated molecule $[M + OH]^+$, and *m/z* 203.2253 to the oxidized and deuterated molecule $[M + OD]^+$. The slightly lower signals for $[M – H]^+$ and $[M + OH]^+$ in D_2O saturated CO_2 atmosphere suggested that the concomitant contribution of protonation by H_3O^+ clusters is increasing, as expected, but still not exclusive.

To further elucidate the $[M + H]^+$ ion formation, we conducted a series of experiments with dry air, using analyte in protic and aprotic deuterated solvents. Therefore, we now have to differentiate between proton and hydrogen sources, since in case of a radical pathway, a hydrogen radical is transferred. For deuterated protic solvents (D_2O, MeOD, EtOD) we did not observe complete deuteration (<76%) of the molecule, which was unexpected, since the solvent should be the only deuterium source in the system (Table 2). This may be explained by some residual water in the system or by alternative proton/hydrogen sources, e.g. impurities or analyte. However, if the solvent was aprotic (benzene-d_6, $CDCl_3$), still 30% of the transferred deuterium atoms originated from these solvents. Here, the remaining hydrogen atoms/protons probably originated from residual water or impurities (e.g. plasticizers) or from other analyte molecules. This finding also supports the radical driven protonation pathway, since $CDCl_3$ or benzene are very unlikely to be incorporated into water clusters and even less unlikely to donate deuterons. In summary, these experiments indicate that for protic solvents (e.g. MeOD, EtOD, etc.) a large fraction of the hydrogen atoms/protons originate from the solvent. The experiment was therefore repeated in humid air (4 % relative humidity) in order to monitor if the water or the

Table 2. The intensity ratio (%) of the deuterated molecules $[M + D]^+$ to the sum of protonated and deuterated molecules ($[M + H]^+ + [M + D]^+$) of tributylamine vaporized from different deuterated solvents under dry (<100 ppm H_2O) and humid (4% relative humidity, at room temperature) air atmosphere was calculated. The numbers were corrected by the natural abundance of ^{13}C and resolution of MS

Air atmosphere	Intensity ratio ($[M + D]^+$/ ($[M + H]^+ + [M + D]^+$)) in different solvents				
	D_2O	MeOD	EtOD	$CDCl_3$	Benzene-D_6
Dry	61.1% ± 1.6%	69.6% ± 1.7%	69.7% ± 3.6%	26.8% ± 8.6%	28.9% ± 4.5%
Humid	6.5% ± 2.6%	7.5% ± 1.7%	5.3% ± 2.3%	1.1% ± 3.8%	3.7% ± 2.5%

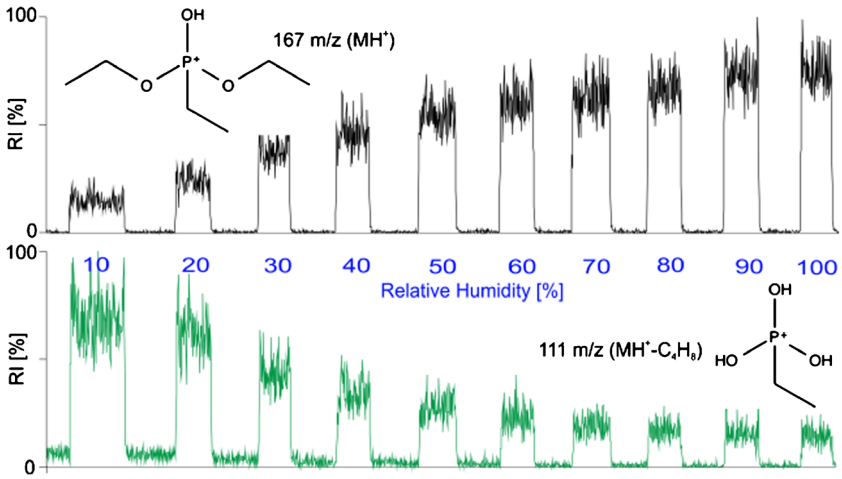

Figure 3. Extracted mass traces of consecutive (1 min) injections of 100 ppb (gas-phase concentration) of diethyl ethylphosphonate. Shown are the protonated molecule (top) and its main in-source fragmentation product (bottom), when operating the active capillary plasma ionization source in air with increasing relative humidity. Measured on an ion trap instrument

solvent is the preferred hydrogen/proton source. Still about 10% of the ions were deuterated in this case (Table 2). Considering the concentration difference (0.13 ppm deuterated solvent versus 792.87 ppm H_2O, at atmospheric pressure and room temperature) this suggests that protic organic solvents (like EtOD) are the preferred hydrogen/proton sources compared to water.

In order to study the effect of the humidity on the $[M + H]^+$ ion formation in more detail, very labile analytes, alkylphosphonates, were measured in water-saturated air atmospheres. We observed a varying in-source fragmentation depending on the humidity of the plasma gas. This provides additional insight into the underlying mechanisms. For phosphonates (e.g., diethyl ethylphosphonate) ionized by the active capillary plasma ionization source, we observed a decreasing in-source fragmentation for increasing plasma gas humidity (Figure 3). The hydronium cluster model can again not explain these findings, since no (or at most, a constant) in-source fragmentation would be expected for proton transfer alone. The increase in in-source fragmentation for decreasing relative humidity was also observed with the flowing atmospheric-pressure afterglow (FAPA) and DART, but has so far not been explained mechanistically[25]. The effect of the humidity may be explained if the ionized analyte ($[M]^{+\bullet}$) is not stable at low humidity and undergoes a fragmentation (McLafferty rearrangement [26]) instead of a protonation ($[M + H]^+$). However, these results have to be carefully assessed since the protonated anlayte ($[M + H]^+$) produces the same fragment ion at *m/z* 111. With increasing amount of protons available for abstraction (higher humidity), the formation of the protonated analyte is favored and therefore the in-source fragmentation is reduced.

Including these and previous findings in a mechanistic model, we propose an additional radical cation pathway for the formation of protonated species in APCI. The proposed radical cation mechanism is highlighted in Scheme 1, which also includes the currently accepted and concomitant hydronium ion/cluster pathway.

Our results provide the following evidence for a significant contribution of a radical-driven ionization mechanism for the formation of $[M + H]^+$ ion in plasma-based, APCI-like ambient ionization methods: (1) $[M + OH]^+$ and $[M - H]^+$ ions are formed when using CO_2 as plasma gas through a radical-driven reaction with $CO_2^{+\bullet}$, (2) the activation energy and the reaction free energy of different radical and non-radical reactions, as calculated by DFT, support our findings, (3) deuterium atoms incorporated in $[M + D]^+$ can originate from aprotic solvents such as chloroform-d and benzene-d_6, (4) the $[M + H]^+$ ion is

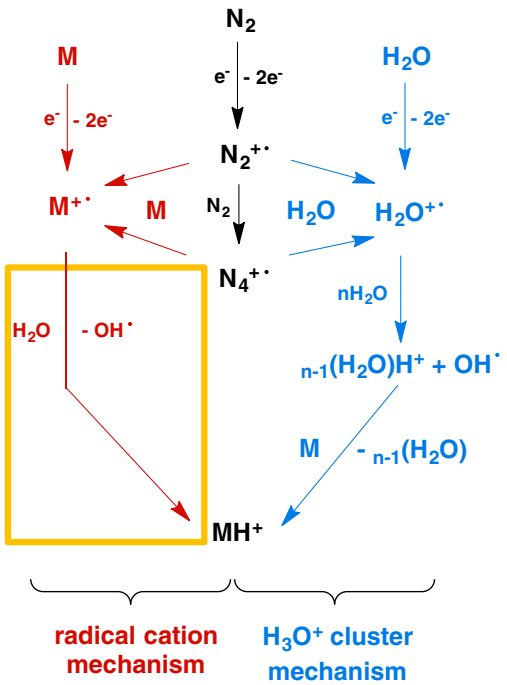

Scheme 1. Main APCI ionization mechanisms to produce protonated analyte ($[M + H]^+$) in a N_2 atmosphere. The part in the yellow box highlights the new contribution to the $[M + H]^+$ ion formation

also formed under dry conditions (no H_3O^+ clusters present), and (5) an in-source fragmentation of diethyl ethylphosphonate was quenched by humidity. This does not contradict, but complements the currently accepted ionization mechanism by hydronium clusters in APCI.

Conclusions

Although our measurements were performed with the active capillary plasma ionization source, these results can be generalized for all plasma-based atmospheric pressure ionization methods (APCI, APPI, DART, FAPA, LTP, etc.), since similar reactive species (i.e., $N_2^{+\bullet}$) are formed in all these methods. Confirmed in various studies by means of spectroscopy, they cause the "glowing" purple color of the plasma, visible by eye. Given the same reactive species as starting point, a similar chemical mechanism can be assumed for all these methods, leading to a reasonable generalization of our findings. Additionally, these reactive species are a common starting point for both pathways to the protonated analyte ($[M + H]^+$): the currently accepted APCI hydronium cluster mechanism and the radical cation pathway revealed in this study. The latter starts with the initial ionization of gas, solvent, and analyte attributable to electron ionization. Subsequently, the radical cations formed react with other neutral molecules or undergo fragmentation to get rid of their excess energy. Depending on the stability of the intermediates, this can lead to in-source fragmentation, in case of insufficient protic collision partners. However, most likely, the intermediates undergo stabilization by hydrogen atom abstraction from other reaction partners such as solvents, leaving mainly a protonated molecule. Depending on the experimental conditions, this pathway may be even more important than proton transfer by hydronium clusters, marking the difference to spray-based ambient ionization methods, which lack this "radical" pathway. Since the contribution of both mechanisms to the final ion yield may vary depending on the solvent content, plasma gas, discharge type, temperature, and chemical properties of each individual compound within the plasma plume, a prediction of the final ionization efficiency for an individual analyte remains challenging. This work adds an additional pathway to the APCI mechanism for the formation of $[M + H]^+$, further elucidating positive ion formation and opening up further possibilities in the prediction of ionization efficiencies.

Acknowledgments

The authors thank Christoph Bärtschi and Christian Marro of the ETH mechanical shop for manufacturing the active capillary plasma ionization source and various other relevant parts. They gratefully acknowledge Dr. Juan Zhang (Novartis AG) for the donation of the LTQ Orbitrap instrument used in this study. This work was funded by the Federal Office for Civil Protection FOCP, SPIEZ LABORATORY (grant 353004332/Stm) that is gratefully acknowledged.

References

1. Xuelu Ding, Y.D.: Plasma-based ambient mass spectrometry techniques: the current status and future prospective. Mass Spectrom. Rev. **34**, 449–473 (2013)
2. Alberici, R.M., Simas, R.C., Sanvido, G.B., Romão, W., Lalli, P.M., Benassi, M., Cunha, I.B.S., Eberlin, M.N.: Ambient mass spectrometry: bringing MS into the "real world.". Anal. Bioanal. Chem. **398**, 265–294 (2010)
3. Horvatic, V., Vadla, C., Franzke, J.: Spectrochimica Acta Part B Discussion of fundamental processes in dielectric barrier discharges used for soft ionization. Spectrochim. Acta B **100**, 52–61 (2014)
4. Marek Smoluch, P.M.S.: Plasma-based ambient ionization mass spectrometry in bioanalytical sciences. Mass Spectrom. Rev. **35**, 22–34 (2015)
5. Kauppila, T.J., Kuuranne, T., Meurer, E.C., Eberlin, M.N., Kotiaho, T., Kostiainen, R.: Atmospheric pressure photoionization mass spectrometry. Ionization mechanism and the effect of solvent on the ionization of naphthalenes. Anal. Chem. **74**, 5470–5479 (2002)
6. Cunningham, A.J., Payzant, D., Kebarle, P.: Kinetic study of the proton hydrate H + (H, O), equilibria in the gas phase. J. Am. Chem. Soc. **94**, 7627–7632 (1972)
7. Klee, S., Derpmann, V., Wißdorf, W., Klopotowski, S., Kersten, H., Brockmann, K.J., Benter, T., Albrecht, S., Bruins, A.P., Dousty, F., Kauppila, T.J., Kostiainen, R., O'Brien, R., Robb, D.B., Syage, J.A.: Are clusters important in understanding the mechanisms in atmospheric pressure ionization? Part 1: reagent ion generation and chemical control of ion populations. J. Am. Soc. Mass Spectrom. **25**, 1310–1321 (2014)
8. Cody, R.B.: Observation of molecular ions and analysis of nonpolar compounds with the direct analysis in real time ion source. Anal. Chem. **81**, 1101–1107 (2009)
9. Kolakowski, B.M., Grossert, J.S., Ramaley, L.: Studies on the positive-ion mass spectra from atmospheric pressure chemical ionization of gases and solvents used in liquid chromatography and direct liquid injection. J. Am. Soc. Mass Spectrom. **15**, 311–324 (2004)
10. Harper, J.D., Charipar, N.A., Mulligan, C.C., Zhang, X., Cooks, R.G., Ouyang, Z.: Low-temperature plasma probe for ambient desorption ionization. Anal. Chem. **80**, 9097–9104 (2008)
11. Andrade, F.J., Shelley, J.T., Wetze, W.C., Webb, M.R., Gamez, G., Ray, S.J., Hieftje, G.M.: Atmospheric pressure chemical ionization source. 1. Ionization of compounds in the gas phase. Anal. Chem. **80**, 2646–2653 (2008)
12. Syage, J.A.: Mechanism of [M + H] + formation in photoionization mass spectrometry. J. Am. Soc. Mass Spectrom. **15**, 1521–1533 (2004)
13. Chen, H., Gamez, G., Zenobi, R.: What can we learn from ambient ionization techniques? J. Am. Soc. Mass Spectrom. **20**, 1947–1963 (2009)
14. Kolakowski, B.M., Grossert, J.S., Ramaley, L.: The importance of both charge exchange and proton transfer in the analysis of polycyclic aromatic compounds using atmospheric pressure chemical ionization mass spectrometry. J. Am. Soc. Mass Spectrom. **15**, 301–310 (2004)
15. Song, L., Gibson, S.C., Bhandari, D., Cook, K.D., Bartmess, J.E.: Ionization mechanism of positive-ion direct analysis in real time: a transient microenvironment concept. Anal. Chem. **81**, 10080–10088 (2009)
16. Herrera, L.C., Grossert, J.S., Ramaley, L.: Quantitative aspects of and ionization mechanisms in positive-ion atmospheric pressure chemical ionization mass spectrometry. J. Am. Soc. Mass Spectrom. **19**, 1926–1941 (2008)
17. Guo, C., Tang, F., Chen, J., Wang, X., Zhang, S., Zhang, X.: Development of dielectric-barrier-discharge ionization. Anal. Bioanal. Chem. **407**, 2345–2364 (2015)
18. Nudnova, M.M., Zhu, L., Zenobi, R.: Active capillary plasma source for ambient mass spectrometry. Rapid Commun. Mass Spectrom. **26**, 1447–1452 (2012)
19. Wolf, J.-C., Schaer, M., Siegenthaler, P., Zenobi, R.: Direct quantification of chemical warfare agents and related compounds at low ppt levels: comparing active capillary dielectric barrier discharge plasma ionization and secondary electrospray ionization mass spectrometry. Anal. Chem. **87**, 723–729 (2015)

20. Wolf, J.-C., Schaer, M., Siegenthaler, P., Zenobi, R.: Direct gas-phase detection of nerve and blister warfare agents utilizing active capillary plasma ionization mass spectrometry. Eur. J. Mass Spectrom. **21**, 305–312 (2015)
21. Gaussian 09, Revision **D.01**, M. J. Frisch, G. W. Trucks, H. B. Schlegel, G. E. Scuseria, M. A. Robb, J. R. Cheeseman, G. Scalmani, V. Barone, B. Mennucci, G. A. Petersson, H. Nakatsuji, M. Caricato, X. Li, H. P. Hratchian, A. F. Izmaylov, J. Bloino, G. Zheng, J. L. Sonnenberg, M. Hada, M. Ehara, K. Toyota, R. Fukuda, J. Hasegawa, M. Ishida, T. Nakajima, Y. Honda, O. Kitao, H. Nakai, T. Vreven, J. A. Montgomery, Jr., J. E. Peralta, F. Ogliaro, M. Bearpark, J. J. Heyd, E. Brothers, K. N. Kudin, V. N. Staroverov, R. Kobayashi, J. Normand, K. Raghavachari, A. Rendell, J. C. Burant, S. S. Iyengar, J. Tomasi, M. Cossi, N. Rega, J. M. Millam, M. Klene, J. E. Knox, J. B. Cross, V. Bakken, C. Adamo, J. Jaramillo, R. Gomperts, R. E. Stratmann, O. Yazyev, A. J. Austin, R. Cammi, C. Pomelli, J. W. Ochterski, R. L. Martin, K. Morokuma, V. G. Zakrzewski, G. A. Voth, P. Salvador, J. J. Dannenberg, S. Dapprich, A. D. Daniels, Ö. Farkas, J. B. Foresman, J. V. Ortiz, J. Cioslowski, and D. J. Fox, Gaussian, Inc., Wallingford CT, 2009.
22. Franklin J.L., Dillard J.G., Rosenstock H.M., Herron J.T., D.K.: Ionization potentials, appearance potentials, and heats of formation of gaseous positive ions. National Bureau of Standards, Washington, D.C. (1969)
23. Chan, G.C.Y., Shelley, J.T., Wiley, J.S., Engelhard, C., Jackson, A.U., Cooks, R.G., Hieftje, G.M.: Elucidation of reaction mechanisms responsible for afterglow and reagent-ion formation in the low-temperature plasma probe ambient ionization source. Anal. Chem. **83**, 3675–3686 (2011)
24. Shelley, J.T., Wiley, J.S., Chan, G.C.Y., Schilling, G.D., Ray, S.J., Hieftje, G.M.: Characterization of direct-current atmospheric-pressure discharges useful for ambient desorption/ionization mass spectrometry. J. Am. Soc. Mass Spectrom. **20**, 837–844 (2009)
25. Newsome, G.A., Ackerman, L.K., Johnson, K.J.: Humidity effects on fragmentation in plasma-based ambient ionization sources. J. Am. Soc. Mass Spectrom. **27**, 135–143 (2015)
26. Snyder, A.P., Harden, C.S.: Determination of the fragmentation mechanisms of organophosphorus ions by water and deuterium oxide atmospheric-pressure ionization tandem mass spectrometry. II. Dialkyl alkylphosphonate ions. Org. Mass Spectrom. **25**, 301–308 (1990)